Polyphenol oxidase mutant *Nicotiana benthamiana* plants increase yield and purity of recombinant proteins and enable studies of proteins in their native state.

Kaijie Zheng and Renier A. L. van der Hoorn*

The Plant Chemetics Laboratory, Department of Biology, University of Oxford, OX1 3RB Oxford

*, for correspondence: renier.vanderhoorn@biology.ox.ac.uk

ORCID IDs: 0000-0001-5773-5962 (KZ), 0000-0002-3692-7487 (RH)

ABSTRACT

Agroinfiltration of *Nicotiana benthamiana* is frequently used to produce recombinant proteins, both for plant science and for molecular pharming. Here, we introduce two genome-edited lines of *N. benthamiana* lacking two polyphenol oxidases (PPOs). These double *ppo* knockout lines grow slightly faster than wild-type and show similar levels of transient GFP expression. However, leaf extracts produced in native buffers stay greener and show much less native crosslinking of Rubisco and other proteins, demonstrating that PPO depletion reduces enzymatic browning and protein crosslinking in leaf extracts. Transient PPO1 expression in the *ppo* mutant restores browning and crosslinking in leaf extracts. These *ppo* mutants offer tremendous opportunities to increase yield and purity of recombinant proteins and study protein complexes, as illustrated with a nearly 4-fold increase in purification yield and a substantial improvement of protein purity upon purification of transiently expressed His-tagged tomato immune protease P69B from total leaf extracts.

INTRODUCTION

Transient protein expression upon agroinfiltration in *Nicotiana benthamiana* is frequently used in plant science and molecular pharming (Beritza et al., 2024). Plant science uses this method routinely e.g. to study the protein-protein interactions (Win et al., 2011) and produce proteins for structural studies (Lawson et al., 2025). Molecular Pharming industry has used this platform e.g. for the production of vaccines against SARS-CoV-2 (Hager et al., 2022) and monoclonal antibodies. All these methods involve the purification of recombinant proteins from total extracts of agroinfiltrated leaves.

We recently discovered that the depletion of polyphenol oxidase (PPO) using virus-induced gene silencing (VIGS) with tobacco rattle virus (TRV) vectors suppresses enzymatic browning and protein crosslinking in leaf extracts of agroinfiltrated *N. benthamiana* (Mahadevan et al., 2025). PPO is a chloroplastic enzyme that oxidises phenolics that are released from the vacuole upon tissue disruption, resulting in reactive quinones that react with themselves and other molecules to form a brown melanin-like polymer (Siu et al., 2023). PPOs can also act as tyosinases by oxidizing solvent-exposed tyrosine residues on proteins into reactive quinones. We recently discovered that the large

subunit of ribulose-1,5-bisphosphate carboxylase/oxygenase (RBCL) shifts into a 200 kDa high molecular weight (HMW) complex in extracts of *TRV::GUS* control plants, but not in extracts of *TRV::PPO* plants (Mahadevan et al., 2025). Thus, extracts of *TRV::PPO* plants show less browning and RBCL crosslinking.

The RBCL crosslinking indicates that also recombinant proteins might get trapped in the polymer during purifications from agroinfiltrated leaves, reducing the yield and purity of recombinant proteins. Here, we introduce two independent genome-edited *ppo* knockout lines that lack the two *PPO* genes that we previously silenced in *TRV::PPO* plants. We investigated these lines for enzymatic browning and native crosslinking and show that these lines improve purification yield and purity of a His-tagged protein, as an example of recombinant proteins.

RESULTS AND DISCUSSION

The 300bp fragment that we previously used to silence *PPO* (Mahadevan et al., 2025) targets two highly homologous *PPO* genes: *PPO1* (NbL17g16540) and *PPO2* (NbL10g18390). To generate the *ppo* knockout lines, we designed two small guide RNAs (sgRNAs) targeting these *PPO* genes and we selected two independent homozygous lines carrying disrupted open reading frames for both genes. Line #1 carries a 284bp deletion in *PPO1* (allele *ppo1-1*), and 2bp and 1bp deletions in *PPO2* (allele *ppo2-1*), whereas line #2 carries a different 284bp deletion in *PPO1* (allele *ppo1-2*) and a 281bp inversion in PPO2 (allele *ppo2-2*) (**Figure 1A**). Consequently, both *PPO1* and *PPO2* were disrupted early in the open reading frames before encoding the catalytic residues (**Figure 1B**), indicating that these lines are double null mutants for both *PPO* genes. Western blot analysis of leaf extracts with anti-PPO antibodies indeed confirmed that both lines lack the PPO protein (**Figure 1C**).

Both *ppo* mutants grew and developed normally (**Figure 2A**), but the *ppo* mutants seemed to grow slightly larger. We therefore also measured the fresh weights of plants in four batches and found that *ppo* mutants indeed accumulate 20-32% more fresh weight (**Figure 2B**), which is a great benefit to protein production yields.

We next monitored native crosslinking and browning in extracts of leaves of three different ages (**Figure 3A**). Western blot analysis revealed that PPO protein accumulates in all leaves and this signal is absent in leaf extracts from both *ppo* mutants (**Figure 3B**). PPO accumulation clearly correlates with leaf age, with most PPO protein accumulating in young, expanding leaves (**Figure 3B**). A Ponceau-S stain of the corresponding membrane to show equal loading also displays a high molecular weight (HMW) signal for WT plants that is absent from *ppo* mutant lines (**Figure 3C**). We previously showed that this HMW signal contains crosslinked RBCL (Mahadevan et al., 2025). This HMW signal is strongest in mature leaves (**Figure 3C**), which are most often selected for agroinfiltration for their high expression and ease of infiltration. The leaf extracts from *ppo* plants generated in TBS were also greener than those of WT (**Figure 3D**). Taken together, these data

demonstrate that PPOs are responsible for both native RBCL crosslinking and for browning in leaf extracts.

Because the leaf extracts of *ppo* mutants not only appeared less brown, but also much greener, we quantified chlorophyll levels in acetone extracts by absorbance. These measurements indicate a significant 68-135% increase of chlorophyll-a and a similar but less significant 57-110% increase of chlorophyll-b (**Figure 4**). This data suggest that both chlorophylls are oxidized by PPO in leaf extracts.

We previously noticed that in some experiments, the transient expression of GFP might be higher in *TRV::PPO* plants (Mahadevan et al., 2025). To test this with our *ppo* mutants, we transiently expressed GFP in both WT and *ppo* mutant plants and analysed leaf extracts for GFP protein levels using anti-GFP western blotting. This revealed that the transient expression level of GFP is not significantly different in *ppo* mutants compared to that of WT plants (**Figure 5**).

To confirm the role of PPO in both native crosslinking and browning, we transiently overexpressed PPO1 and the empty vector (EV) control by agroinfiltrating the *ppo* mutant. Western blot analysis confirmed that PPO accumulated in leaves agroinfiltrated with *35S:PPO* and not in the EV control (**Figure 6A**). Ponceau-S staining revealed that the HMW signal accumulated upon PPO expression when extracts were generated in TBS (**Figure 6B**). However, this HMW signal did not appear when extractions were done directly in gel loading buffer (GLB) containing reducing agent dithiothreitol (DTT) and sodium dodecyl sulphate (SDS) (**Figure 6B**), indicating that protein crosslinking occurs during extraction and that PPO inactivation can prevent this. Extracts of *ppo* mutant leaves transiently expressing PPO1 also turn brown, in contrast to those of the EV-infiltrated *ppo* mutant (**Figure 6C**).

Because native crosslinking occurs during protein extraction in TBS, which is frequently used to study proteins in their native state, we tested if protein purification is improved when extracting transiently expressed recombinant proteins from *ppo* mutants. We previously established an efficient procedure of His-tagged proteins from agroinfiltrated leaves (Schuster et al., 2022). We followed this protocol to purify His-tagged P69B, a defence-related subtilase of tomato that we study as a target for various pathogen-secreted proteins (Homma et al., 2023). Transient expression of P69B-His resulted in similar levels of P69B accumulation between WT and *ppo* mutant plants (**Figure 7A**). Also the capture on the Ni-NTA beads is similar (**Figure 7A**). The P69B-His level in the eluate, however, is nearly 4-fold higher when extracted from *ppo* plants when compared to WT plants (**Figure 7A**), indicating a drastic improvement in purification yield of P69B-His.

The Ponceau-S staining revealed that the HMW signal is absent in extracts of *ppo* plants but is present in the flow-through, indicating that some native crosslinking occurs during the incubation with the beads, even in extracts of the *ppo* mutant (**Figure 7B**). The HMW signal is also present in the eluate of WT plants, but much less in that of *ppo* mutant plants (**Figure 7B**), indicating that eluates from *ppo* plants are much cleaner when compared to those from WT plants.

CONCLUSION

We have introduced two independent *ppo* double mutant lines and showed that these lines lack the PPO protein, and have less native crosslinking and browning in leaf extracts. Transient GFP expression is not affected in *ppo* mutants, but the purification yield of P69B is significantly improved. These data indicate that these *ppo* lines will be instrumental for both plant science and molecular pharming industry by enabling the production and study purified proteins in their native state *in planta*.

MATERIALS & METHODS

Plants materials and growth conditions - *N. benthamiana* LAB was transformed with a T-DNA carrying Cas9 and two single guide RNAs targeting each gene (**Supplemental Table S1**). Two independent CRISPR mutants were identified as homozygous by PCR and sequencing using sequencing primers listed in **Supplemental Table S1**. The plants were maintained in a controlled growth room environment at 22 °C. The plants were exposed to a 16-h light/8-h dark photoperiod, under an illumination intensity of 2000 cd·sr·m□².

Agroinfiltration - *Agrobacterium tumefaciens* GV3101 (pMP90) was used for agroinfiltration. Agrobacterium cultures were grown overnight in LB medium supplemented with 50 µg/ml kanamycin, 10 µg/ml gentamicin and 50 µg/ml rifampicin at 28 °C with shaking at 200 rpm. For transient protein expression assays, overnight cultures of Agrobacterium strains carrying binary vectors listed in Supplemental **Table S2** were harvested by centrifugation. Bacterial pellets were resuspended in infiltration buffer (10 mM MgCl□, 10 mM MES, pH 5.6, 150 µM acetosyringone) and mixed at a 1:1 ratio with Agrobacterium harboring the silencing suppressor p19, with each strain adjusted to an OD□□□ of 0.5. After incubation at 28 °C for 1 h, bacterial suspensions were infiltrated into leaves of 4-week-old *Nicotiana benthamiana* plants. Inoculated plants were maintained in a growth chamber until further use.

Molecular cloning - To generate a plasmid encoding PPO1 flanked by FLAG and His tags, total RNA was extracted from leaves of ~4-week-old wild-type *Nicotiana benthamiana* plants (FastPure Universal Plant Total RNA Isolation Kit, RC411-01, Vazyme), and the full-length open reading frame (ORF) of *PPO1* was amplified (Q5® Hot Start High-Fidelity DNA Polymerase, M0493S, NEB) by reverse transcription PCR (RT-PCR). The amplified ORF was subsequently recombined into a vector containing the 35S promoter, an N-terminal FLAG tag (Zheng et al., 2024), and a C-terminal His tag using ClonExpress Ultra One Step Cloning Kit V2 (C116-02, Vazyme), resulting in pKZ205.

SDS-PAGE and Western blot - For total protein extraction from *Nicotiana benthamiana* leaves, samples were rapidly frozen in liquid nitrogen and ground to a fine powder with glass beads using a homogenizer. Depending on the experimental requirements, TBS or 2× gel loading buffer was added. When total protein was extracted using TBS, 4× gel loading buffer was subsequently added for SDS–PAGE analysis. After addition of the loading buffer, samples were denatured at 98 °C for 5 min and then loaded onto 12% SDS–PAGE gels and electrophoresed at 180 V in Invitrogen Novex vertical gel tanks. PageRuler™ Prestained Protein Ladder, 10 to 180 kDa (26616, Thermo Scientific™) was used as the protein ladder. Proteins were transferred to PVDF membranes using a BIO-RAD transfer apparatus and kit (Trans-Blot Turbo RTA Midi 0.45 µm LF PVDF Transfer Kit, 1704275), following the manufacturer's instructions. Membranes were blocked in 5% skim milk in PBS-T (PBS tablets, 524650, Merck; 0.1% Tween-20, P1379, Merck) at room temperature for 1 h and then incubated overnight at 4 °C with primary antibodies against PPO (MBS9458497, MyBioSource) and GFP (Ab6663, Abcam), diluted 1:5000 in PBS-T. For PPO detection, membranes were further incubated with goat anti-mouse secondary antibody. Membranes were washed three times with PBS-T for 5 min each, followed by one wash with PBS for 5 min. Signals were developed using SuperSignal™ West Femto Maximum Sensitivity Substrate (34096, Thermo Scientific™) and detected with ImageQuant® LAS-4000 imager (GE Healthcare, Healthcare Life Sciences, Little Chalfont, UK).

P69B-His purification - Total protein was extracted from agroinfiltrated leaves expressing P69B-His using phosphate-buffered saline (PBS). The P69B-His protein was incubated with Ni-NTA Agarose (30210, Qiagen) at 4 °C overnight, washed three times with wash buffer (50 mM Tris-HCl, pH 7.5, 150 mM NaCl, 50 mM imidazole), and subsequently eluted using elution buffer (50 mM Tris-HCl, pH 7.5, 150 mM NaCl, 250 mM imidazole) to recover the purified protein.

ACKNOWLEDGEMENTS

We thank Ursula Pyzio for excellent plant care and Sarah Rodgers, Caroline O'Brien and Patricia Bowman for technical support.

Funding - This project was financially supported by BBSRC project BB/Y00969X/1 (KZ) and ERC project 101019324 (RH).

Author contributions - RH conceived the project; KZ performed the experiments; RH wrote the manuscript with input from KZ.

Competing interests - none declared.

REFERENCES

Beritza K, Watts EC, van der Hoorn RAL. (2024) Improving transient protein expression in agroinfiltrated Nicotiana benthamiana. *New Phytol.* **243**: 846-850.

Homma F, Huang J, van der Hoorn RAL. (2023) AlphaFold-Multimer predicts cross-kingdom interactions at the plant-pathogen interface. *Nat Commun.* **14**: 6040.

Hager KJ, Pérez Marc G, Gobeil P, Diaz RS, Heizer G, Llapur C, Makarkov AI, Vasconcellos E, Pillet S, Riera F, Saxena P, Geller Wolff P, Bhutada K, Wallace G, Aazami H, Jones CE, Polack FP, Ferrara L, Atkins J, Boulay I, Dhaliwall J, Charland N, Couture MMJ, Jiang-Wright J, Landry N, Lapointe S, Lorin A, Mahmood A, Moulton LH, Pahmer E, Parent J, Séguin A, Tran L, Breuer T, Ceregido MA, Koutsoukos M, Roman F, Namba J, D'Aoust MA, Trepanier S, Kimura Y, Ward BJ (2022) CoVLP Study Team. Efficacy and safety of a recombinant plant-based adjuvanted Covid-19 vaccine. *N Engl J Med.* **386**: 2084-2096.

Lawson AW, Macha A, Neumann U, Gunkel M, Chai J, Behrmann E, Schulze-Lefert P. (2025) Purifying recombinant proteins from *Nicotiana benthamiana* for structural studies. *Nat Protoc.* in press

Mahadevan C, Watts EC, Zheng K, Song SJ, van der Hoorn RAL. (2025) Polyphenol oxidase silencing avoids protein cross-linking and enzymatic browning in *Nicotiana benthamiana* leaf extracts. *Plant Biotechnol J.* Jun 18.

Schuster M, Paulus JK, Kourelis J, van der Hoorn RAL. (2022) Purification of His-tagged proteases from the apoplast of agroinfiltrated *N. benthamiana*. *Methods Mol Biol.* **2447**: 53-66.

Sui X, Meng Z, Dong T, Fan X, Wang Q. (2023) Enzymatic browning and polyphenol oxidase control strategies. *Curr. Opin. Biotechnol.* **81**:102921.

Win J, Kamoun S, Jones AM. (2011) Purification of effector-target protein complexes via transient expression in *Nicotiana benthamiana. Methods Mol Biol.* **712**:181-94.

Zheng K, Lyu J, Thomas EL, Schuster M, Sanguankiattichai N, Ninck S, Kaschani F, Kaiser M, van der Hoorn RAL. (2024) The proteome of *Nicotiana benthamiana* is shaped by extensive protein processing. *New Phytol*. **243**: 1034-1049.

FIGURES

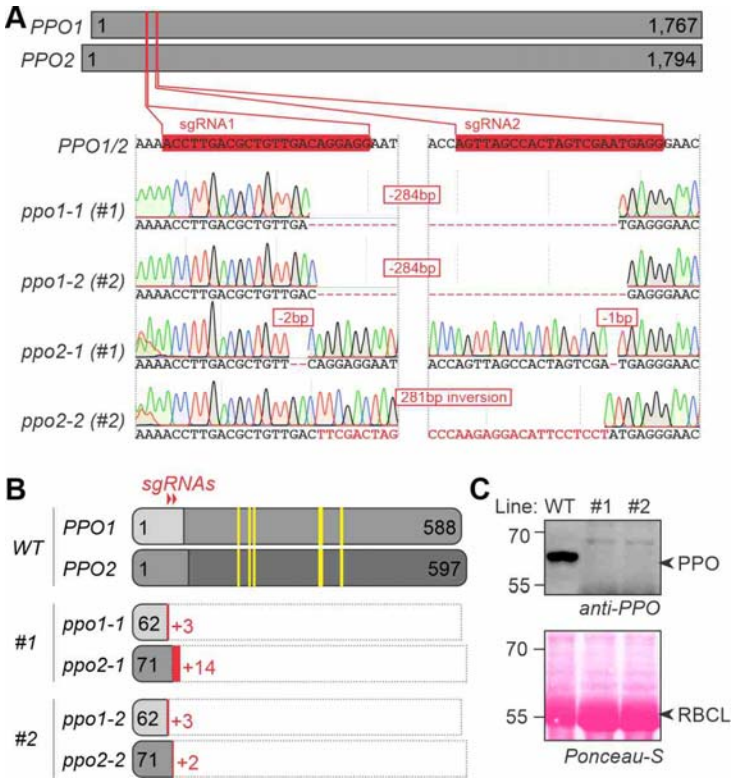

Figure 1 Two independent *ppo* double mutant knockout lines.

(A) CRISPR/Cas9-induced nucleotide alterations in *PPO* genes. The 5' region of the open reading frames of *PPO1* and *PPO2* were targeted by two small guide RNAs (sgRNAs, red). The sgRNA target locus were sequenced in homozygous lines #1 and #2 carrying alleles *ppo1-1* and *ppo2-1* in line #1 or alleles *ppo1-2* and *ppo2-2* in line #2, respectively. Shown are the alignments with wild-type *PPO1* and *PPO2*, which are identical in the shown regions. **(B)** Predicted proteins encoded by the mutant *ppo* alleles. The length of the open reading frame including the nonsense sequence (red) is indicated in amino acid residues. The prodomain (light grey) and catalytic residues (yellow) are highlighted. **(C)** The PPO protein is absent in leaf extracts of *ppo* mutants. Leaf extracts from 4-week-old plants were analysed by Ponceau-S staining and western blot analysis using the anti-PPO antibody.

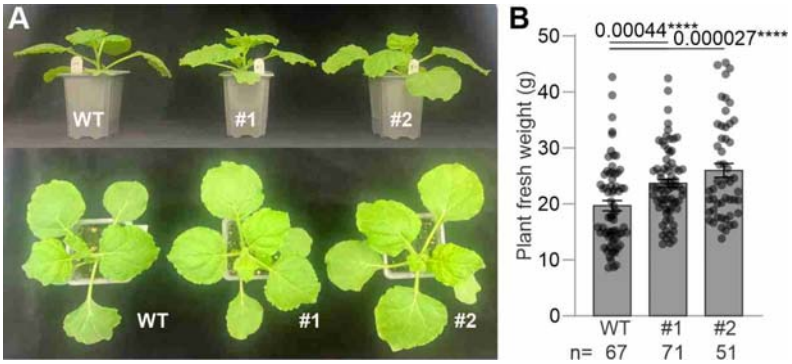

Figure 2 Both *ppo* mutants develop normally and grow slightly better.

(A) 28-day old WT and *ppo* mutant plants. **(B)** Mutant *ppo* plants are slightly larger than wild-type plants. The fresh weight of the plants above ground was measured in four sets of 30-31 days old plants. Error bars represent standard error of n>50 replicates generated in four batches of plants. Statistical significance was assessed using Student's t-test.

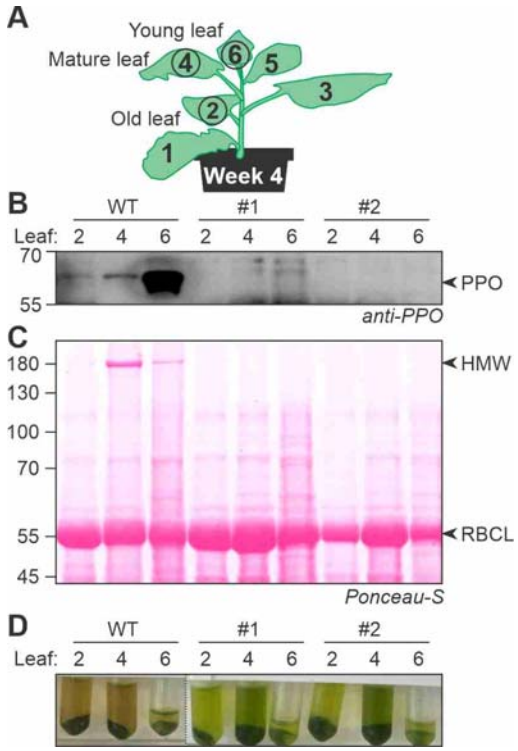

Figure 3 Less native crosslinking and extract browning in both *ppo* mutants.

(A) Position of analysed leaves in a 4-week-old *N. benthamiana* plant. **(B)** PPO accumulates more in young leaves and is absent in *ppo* mutants. **(C)** Native crosslinking into high molecular weight (HMW) complexes is absent in *ppo* mutants and more in mature leaves. **(D)** Extract browning is absent in *ppo* mutants. Leaf extracts were extracted in TBS, centrifuged for 2 minutes at room temperature and imaged soon after. **(B-C)** Leaf extracts were generated from 9 (old/mature leaf-2/4) or 3 leaf discs (young leaf-6) in TBS and analysed by Ponceau-S staining and western blot analysis using the anti-PPO antibody.

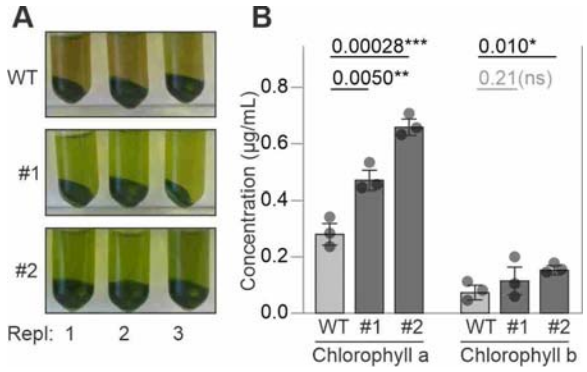

Figure 4 Extracts of *ppo* mutants have higher chlorophyll levels.

Leaf extracts were incubated with acetone and the concentrations of Chlorophyll a and b were measured by absorbance spectroscopy. Error bars represent standard error of n=3 biological replicates. P-values were calculated with the Students *t*-test.

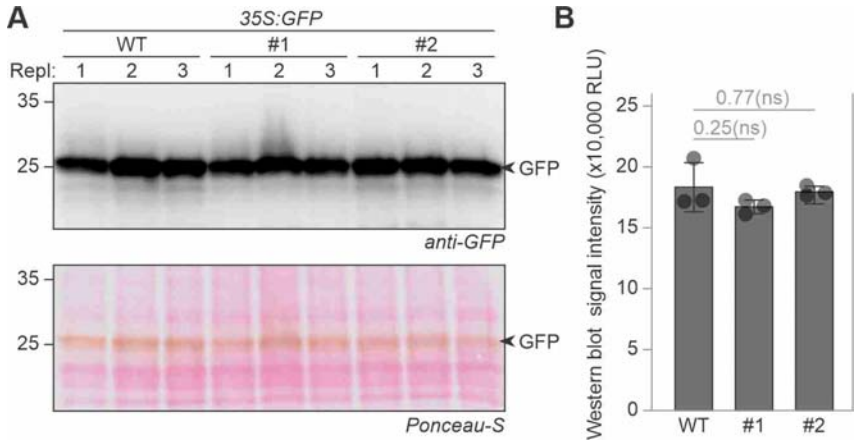

Figure 5 Transient GFP expression is similar in *ppo* lines.

GFP was transiently expressed by agroinfiltration of WT and *ppo* mutant plants. Leaf extracts were generated at day 3 and analysed by anti-GFP western blot and Ponceau-S staining in n=3 biological replicates.

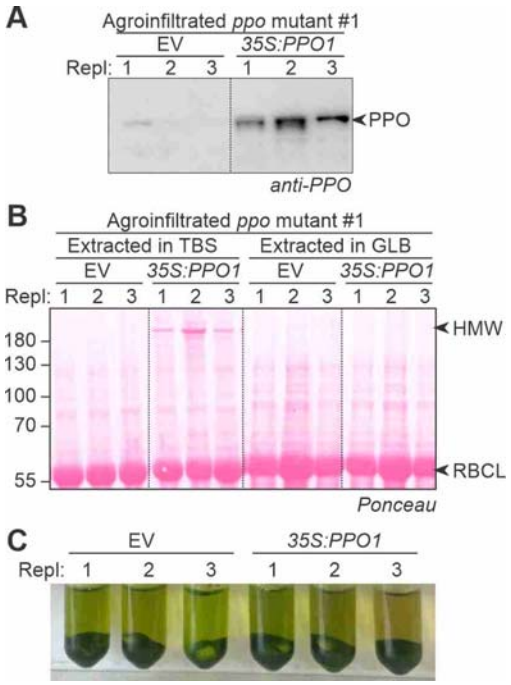

Figure 6 Transient *PPO1* overexpression causes native crosslinking and extract browning. **(A)** PPO1 accumulates in agroinfiltrated leaves. Leaves of the *ppo* mutant #1 were agroinfiltrated and samples were analysed 4 days later by western blot using the anti-PPO antibody. **(B)** Native crosslinking into the HMW complex occurs in extracts of PPO1 expressing leaves in Tris-buffered saline (TBS), but not in gel-loading buffer (GLB). **(C)** Extract browning is promoted by PPO1 overexpression. Leaf extracts in TBS were centrifuged shortly before picture was taken.

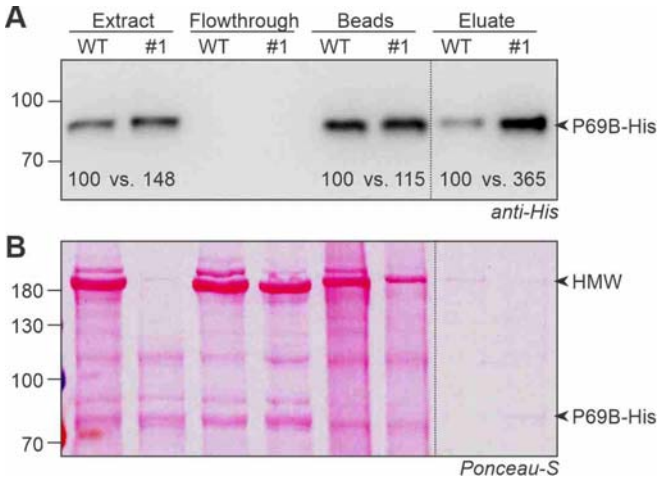

Figure 7 Increased purification efficiency of P69B-His from *ppo* mutant plants.

(A) More P69B-His was purified from the *ppo* mutant. **(B)** Native crosslinked HMW complexes stick to beads during P69B-His purification from WT plants. **(A-B)** WT and *ppo* mutant line #1 were agroinfiltrated to transiently express P69B-His. Leaf extracts were generated 3 days later and passed over Ni-NTA beads. Beads were washed and eluted with imidazole and samples were analysed by western blot using the PPO-antibody and Ponceau-S staining. Western blot signals were quantified and normalized to the WT signal.

SUPPLEMENTAL TABLES

Table S1 Used oligonucleotides

Name	Sequence (5'-3')
PPO1-F1	GATGACGACGATAAGCTTAAGATGGCTTCTTCTTCTACTTTACCTTTATG
PPO1-R1	ATGGTGATGGTGATGTCTAGAACAATCGACAAGCTTAATCTCAACAC
sgRNA1	ACCTTGACGCTGTTGACAGGAGG
sgRNA2	AGTTAGCCACTAGTCGAATGAGG
PPO1-seq-F1	CAGCAATGGCTTCTTCTTCTACTTT
PPO1-seq-R1	CTTGTAGCTCTTTGCCACCA
PPO2-seq-F2	CCAGCACCAACTCATCTTTCT
PPO2-seq-R1	GGTGACTTTGGTTACGTCTTGC

Table S2 Used plasmids

Name	Description	Reference
pFH20	Binary vector 35S:NtPR1a-P69B-His	Homma et al., 2023
pKZ165	Binary vector 35S:nlsGFP	This work
pKZ205	Binary vector 35S:FLAG-PPO1-2xHis	This work
pJK001c	Empty binary vector	Paulus et al., 2020
P19	Binary 35S::P19	Van der Hoorn et al., 2003

Supplemental references:

Paulus JK, Kourelis J, Ramasubramanian S, Homma F, Godson A, Hörger AC, Hong TN, Krahn D, Ossorio Carballo L, Wang S, Win J, Smoker M, Kamoun S, Dong S, van der Hoorn RAL. (2020) Extracellular proteolytic cascade in tomato activates immune protease Rcr3. *Proc Natl Acad Sci USA.* **117**: 17409-17417.

Van Der Hoorn RAL, Rivas S, Wulff BB, Jones JDG, Joosten MHAJ. (2003) Rapid migration in gel filtration of the Cf-4 and Cf-9 resistance proteins is an intrinsic property of Cf proteins and not because of their association with high-molecular-weight proteins. *Plant J.* **35**: 305-315.